Proceedings of the 21st ICSMGE, Vienna, Austria, 14 – 19 June 2026. Pistrol, Adam & Schweiger (eds.)
Published by: ÖGG, Austrian Society for Geomechanics, Salzburg, Austria, ISBN 978-3-9503898-4-5
https://doi.org/10.53243/ICSMGE2026-2308

Multi-directional shear wave measurement during triaxial compression test of saturated sand using disk-shaped piezoelectric transducer

Hiroyuki Hashimoto, Reiko Kuwano
Institute of Industrial Science, The University of Tokyo, Tokyo, Japan, hsmt@iis.u-tokyo.ac.jp

ABSTRACT: The precise measurement of elastic wave velocity and hence, small-strain stiffness of soil is essential for the design of geotechnical structures. Piezoelectric transducers have been employed for elastic wave measurement, and wave velocity and stiffness anisotropy have also been investigated by installing transducers in the horizontal direction. However, installing and sealing transducers in the horizontal direction is generally challenging, and evaluations of shear (S-) wave velocities and their anisotropy in sheared soils have been mostly limited to small strain levels prior to failure under drained conditions. In this study, an automated multi-directional S-wave velocity measurement system using disk-shaped piezoelectric transducers was developed, which enables easy sealing and quick, non-invasive experimental procedures. The system was applied to saturated Toyoura sand to investigate the evolution of S-wave velocities in multiple directions up to large strains, under both drained and undrained conditions. S-wave velocities exhibited direction-dependent evolution during triaxial compression. The relationship between void ratio-corrected S-wave velocity and geometric mean stress at the end of triaxial compression lay on a single straight line, regardless of the drainage condition or initial relative density. Furthermore, the S-wave velocity ratio, which characterises S-wave velocity anisotropy, remained nearly constant across all tested cases. These findings suggest that the evolution of elastic wave velocities and their anisotropy during triaxial compression is governed by the stress state and tends to converge toward a consistent residual state regardless of initial relative density or drainage condition.

KEYWORDS: Shear wave velocity, triaxial compression test, anisotropy.

1 INTRODUCTION

The precise measurement of elastic wave velocity, and thus the small-strain stiffness of soils, is essential for the design of foundations, earth dams, and other geotechnical structures. Owing to their ease of installation, piezoelectric transducers such as bender elements (BEs) are widely used to measure shear (S-) wave velocities (V_s) of soils. Planar disk-shaped piezo-electric transducers (Suwal & Kuwano, 2013) offer several advantages over BEs, including non-invasiveness, the ability to generate planar waves, and broader applicability to materials such as coarse granular soils and cement-treated soils. These transducers are typically embedded in pedestals and caps to measure vertically propagating S-waves in triaxial specimens. Horizontal installation has also been employed to evaluate inherent and stress-induced anisotropy (Kuwano & Jardine 2002; Dutta et al., 2020a). However, horizontal installation of the transducers required creating openings in the membrane and adhesive bonding, which are time-consuming and sometimes hinder complete sealing. Furthermore, previous studies on multi-directional S-wave measurements have mostly been limited to small-strain levels before failure under drained conditions. To address these limitations, this study aimed to develop a system for multi-directional S-wave measurements using DTs, with improved sealing performance and reduced testing time. The developed system was applied in triaxial compression tests on saturated Toyoura sand, and the evolution of V_s in multiple directions was investigated at large strains, either beyond the peak strength or along the critical state line, under both drained and undrained conditions.

2 METHODOLOGY

2.1 *Multi-directional elastic wave measurement system*

Figure 1 shows the multi-directional elastic wave measurement system developed in this study. Horizontal DTs, used for excitation and measurement of elastic waves propagating horizontally, were fabricated by bonding the back of a shear (S-) type piezoelectric element (20 mm in diameter and 2 mm thick) to the inside of an aluminium housing, using epoxy resin. Silicone was filled around the sides of the element to prevent constraint on its deformation. A custom-made membrane with four cylindrical holes matching the diameter of the horizontal DTs was used, and the DTs were sealed with vacuum grease and O-rings. Specimens were then prepared using a 3D-printed mould. DTs for measuring vertically propagating elastic waves were embedded in the pedestal and top cap (Dutta et al., 2020b). Elastic wave measurements were fully automated through computer control of the function generator, oscilloscope, and coaxial channel switchers. This system eliminates the need to cut the membrane and insert or glue piezoelectric elements, thereby avoiding specimen disturbance and enabling faster and simpler testing. The multi-directional elastic wave measurement system developed in this study enables measurement of three components of S-wave velocity: $V_{s,vh}$, $V_{s,hv}$, and $V_{s,hh}$. In this notation, the first subscript after the comma indicates the direction of wave propagation, and the second indicates the direction of wave oscillation. A single-cycle 7 kHz sine wave was used as the input waveform for S-wave measurements. Travel times were calculated using the Start-to-Start method, as shown in Figure 2.

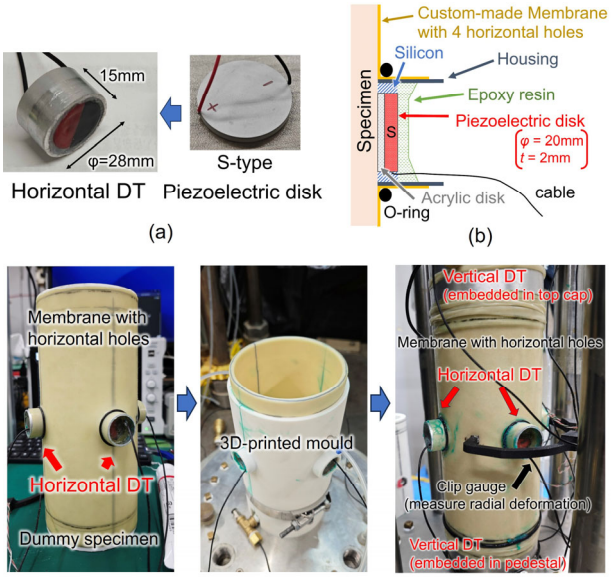

Figure 1. Multi-directional elastic wave measurement system using DTs: (a) horizontal DT, (b) lateral cross-sectional view of horizontal DT, (c) specimen preparation procedure.

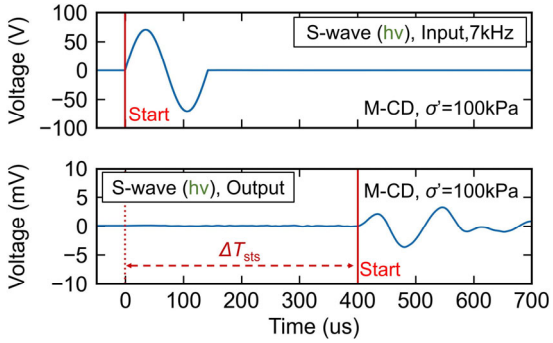

Figure 2. Time-domain response of an S-wave propagating horizontally and oscillating vertically during isotropic consolidation.

Table 1. Summary of triaxial compression tests.

Case name	Initial void ratio	Initial relative density (%)	Drainage condition during compression
L-CD	0.876	26.6	Drained
M-CD	0.786	51.0	Drained
D-CD	0.661	84.9	Drained
L-CU	0.877	26.8	Undrained
M-CU	0.777	53.4	Undrained
D-CU	0.658	85.6	Undrained

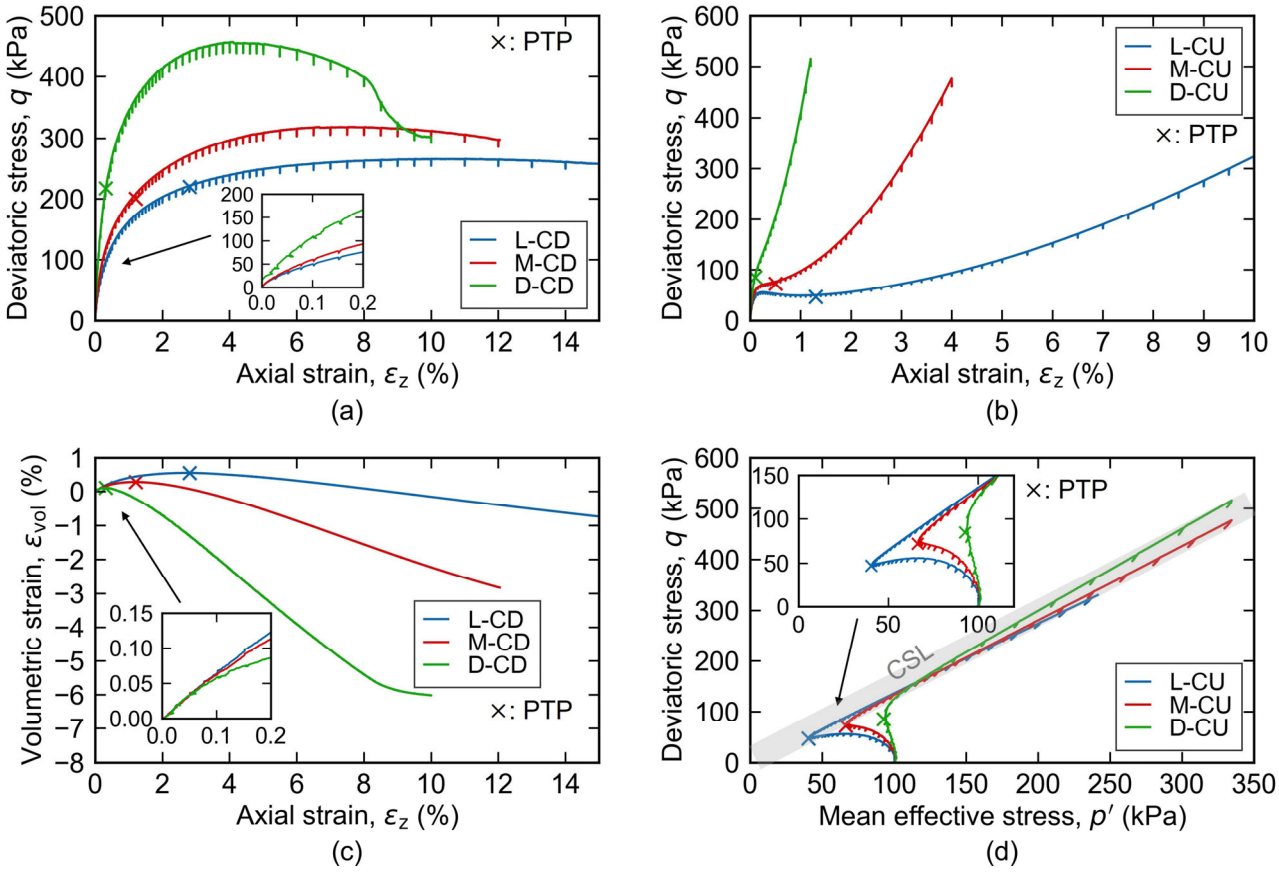

Figure 3. Stress strain responses during triaxial compression tests.

2.2 *Testing program*

S-wave velocities were measured in multiple directions using the developed setup during drained triaxial compression tests on saturated Toyoura sand ($\rho_s = 2.646$, $e_{max} = 0.975$, $e_{min} = 0.605$, $D_{50} = 0.18$ mm). A summary of the test cases is presented in Table 1. Specimens with a height of 180 mm and a diameter of 100 mm were prepared by air-pluviation method. Three types of specimens with different initial relative densities were prepared by varying the sand drop height. Specimens were saturated using the double vacuum method, followed by the application of a back pressure of 200 kPa. After isotropic consolidation under a confining pressure of 100 kPa, specimens were subjected to triaxial compression under drained or undrained conditions at an axial strain rate of 0.2%/min. Multi-directional S-wave measurements were conducted at each stage of consolidation and triaxial compression by temporarily pausing loading.

3 RESULTS AND DISCUSSIONS

3.1 *S-wave velocities with axial strain*

Figure 3 shows the stress–strain relationships during triaxial compression, and Figure 4 presents the variations of S-wave velocity with axial strain. The temporary stress drops observed in the stress–strain curves are attributed to stress relaxation caused by up to 10-second pauses in loading for S-wave measurements. In the drained triaxial compression (CD) tests, $V_{s,hh}$ decreased with axial compression, while $V_{s,vh}$ and $V_{s,hv}$ peaked at the phase transformation point (PTP) and subsequently decreased with strain softening. Each component of the S-wave velocity tended to converge to a direction-specific value, regardless of the initial relative density. In the undrained triaxial compression (CU) tests, all S-wave velocities decreased up to the phase transformation point and then increased after reaching the critical state line (CSL) on the stress path, as effective stress continued to increase.

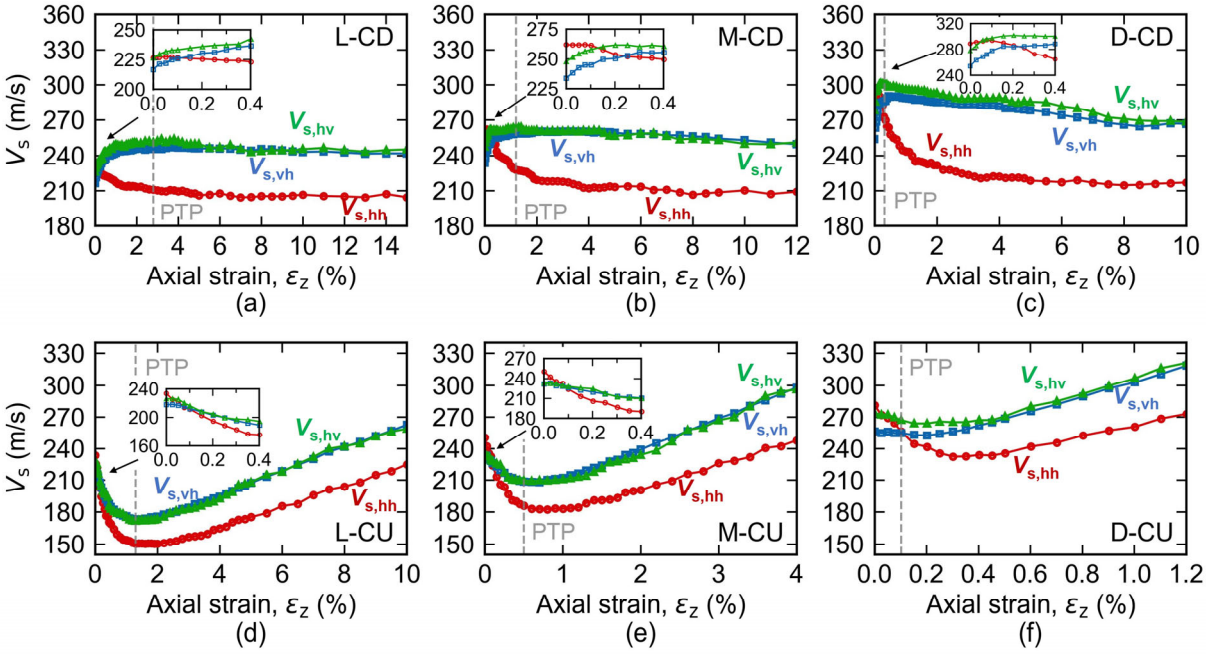

Figure 4. Variations of S-wave velocities (V_s) with axial strain (ε_z).

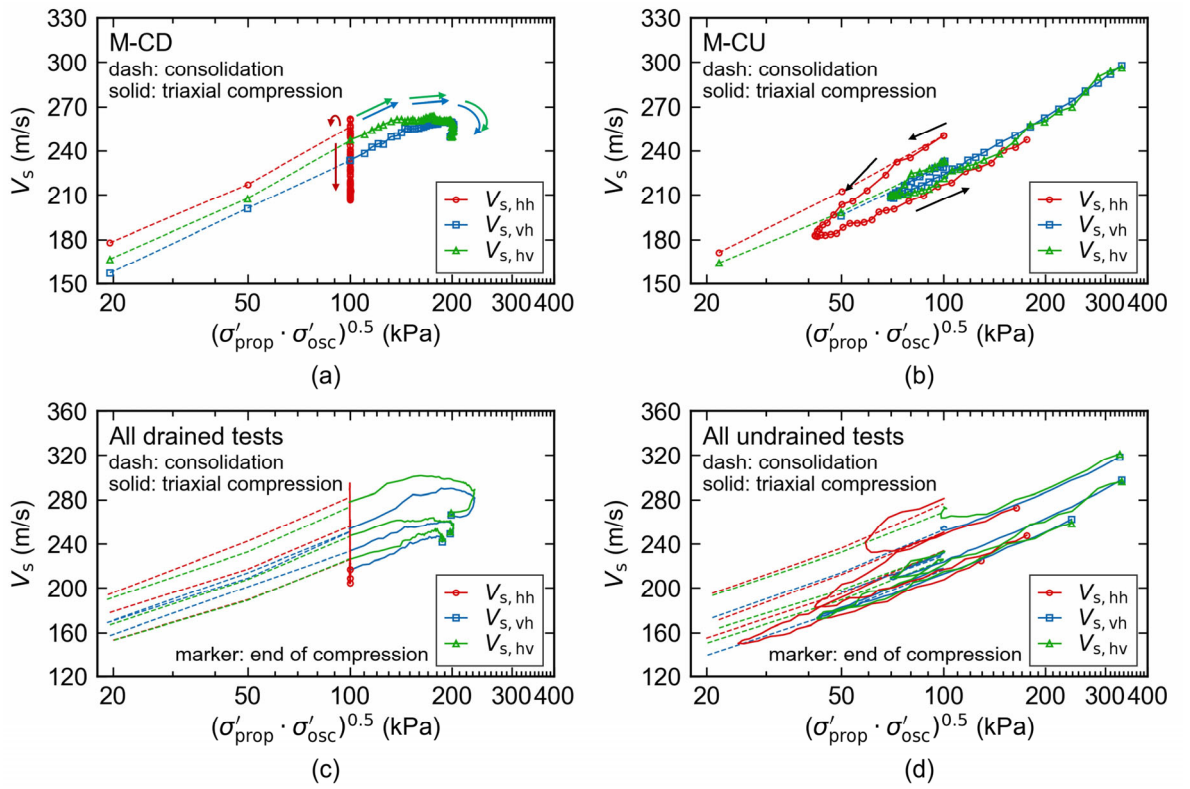

Figure 5. Evolution of S-wave velocity (V_s) with geometric mean stress during isotropic consolidation and triaxial compression.

3.2 *S-wave velocities with geometric mean stress*

Recognising that the S-wave velocities are influenced by the effective stress in both propagation (σ_{prop}') and oscillation (σ_{osc}') directions, they are plotted against the corresponding geometric mean stress. Figure 5 (a) and (b) show the relationships between S-wave velocities and geometric mean stress for the medium dense specimens. In the CD test, $V_{s,hh}$ showed a slight increase during the initial loading stage (at axial strains below approximately 0.1%), followed by a continuous decrease. $V_{s,vh}$ and $V_{s,hv}$ initially followed the same linear trend as in isotropic consolidation, but their rates of increase declined with further loading and eventually shifted to a decreasing trend. In the CU tests, all three S-wave velocities initially decreased along the linear trend observed during isotropic consolidation. As geometric mean stress continued to decrease, the rate of decrease in S-wave velocities increased. Eventually, S-wave velocities began to increase along a single linear trend with the increase of geometric mean stress, regardless of the wave propagation and oscillation directions.

Figure 5 (c) and (d) show the relationships between S-wave velocities and geometric mean stress for all initial relative density cases. In the CD tests, S-wave velocities tended to converge to direction-specific values for each propagation and oscillation direction, regardless of the initial relative density. In the CU tests, by contrast, all cases exhibited a tendency for S-wave velocities to increase along a single linear trend, regardless of propagation or oscillation direction. However, the specific trend lines differed among the cases, appearing as parallel lines. This behaviour may be related to differences in void ratio among the cases. Figure 6 shows the relationship between S-wave velocity normalised by a void ratio correction function and the geometric mean stress. The correction function $f(e) = 2.17 - e$ was adopted following the formulation proposed by Hardin and Richart (1963). Regardless of the initial relative density, drainage condition, or propagation and oscillation directions of the S-waves, all cases at the end of triaxial compression fell on the same line in the relationship between normalised S-wave velocities and the geometric mean stress. This observation suggests that applying a void ratio correction enables a consistent interpretation of S-wave velocities across different directions when the specimens reached the CSL.

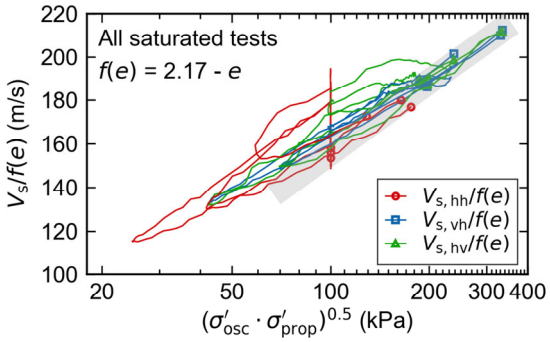

Figure 6. Evolution of void ratio normalised S-wave velocity ($V_s/f(e)$) with geometric mean stress during triaxial compression.

3.3 *S-wave velocities ratio with axial strain*

Figure 7 shows the relationship between the S-wave velocity ratio ($V_{s,hh}/V_{s,hv}$) and axial strain. Following the findings of Liu et al. (2022), which demonstrated that S-wave velocities can be affected by boundary conditions, this study focuses on the comparison between $V_{s,hh}$ and $V_{s,hv}$, as they were subject to identical boundary conditions. At the onset of triaxial compression (under isotropic stress conditions), $V_{s,hh}$ was slightly greater than $V_{s,hv}$, indicating the existence of initial fabric anisotropy. A reduction in the S-wave velocity ratio was observed with increasing axial strain, indicating the development of stress-induced anisotropy. Eventually, the ratio converged to an approximately constant value, regardless of the drainage condition or initial relative density.

4 CONCLUSION

In this study, an automated multi-directional elastic wave measurement system using disk-shaped piezoelectric transducers was developed. The system enabled simplified sealing and a substantial reduction in testing time. Using the developed system, the evolution of S-wave velocities during triaxial compression of saturated Toyoura sand was measured in multiple directions up to large axial strains beyond the peak strength in CD tests and reaching and moving along the CSL in CU tests. In the CD tests, $V_{s,hh}$ decreased continuously with increasing axial strain, whereas $V_{s,vh}$ and $V_{s,hv}$ peaked at the PTP and subsequently declined. In the CU tests, all S-wave velocities decreased until reaching the PTP, after which they began to increase. The relationship between void ratio-corrected S-wave velocity and geometric mean stress at the end of triaxial compression lay on a single straight line. Furthermore, the S-wave velocity ratio, representing anisotropy in S-wave velocity, remained nearly constant, regardless of the drainage condition or initial relative density. These findings suggest that the evolution of S-wave velocities and their anisotropy during triaxial compression is strongly influenced by the stress state and tends to converge toward a consistent residual state.

5 ACKNOWLEDGEMENTS

This work was supported by JSPS KAKENHI Grant Number 25KJ0940. The authors would like to thank Mr. Makoto Kuno of the Institute of Industrial Science, University of Tokyo, for his support during the development of the experimental setup.

6 REFERENCES

Dutta, T.T., Otsubo, M., Kuwano, R., Sato, T. 2020a. Estimating multidirectional stiffness of soils using planar piezoelectric transducers in a large triaxial apparatus. *Soils and Foundations* 60(5), 1269-1286.

Dutta, T.T., Otsubo, M., Kuwano, R., O'Sullivan, C. 2020b. Evolution of shear wave velocity during triaxial compression. *Soils and Foundations* 60(6), 1357-1370.

Hardin, B.O., and Richart, F.E. 1963. Elastic wave velocities in granular soils. *Journal of Soil Mechanics and Foundations Division* 89(1), 33-65.

Kuwano, R., and Jardine, J.R. 2002. On the Applicability of Cross-Anisotropic Elasticity to Granular Materials at Very Small Strains, *Geotechnique* 52(10), 727-749.

Liu, J., Otsubo, M., Kawaguchi, Y., and Kuwano, R. 2022. Anisotropy in small-strain shear modulus of granular materials: Effects of particle properties and experimental conditions. *Soils and Foundations* 62(1), 101105.

Suwal, L.P., and Kuwano, R. 2013. Disk shaped piezo-ceramic transducer for P and S wave measurement in a laboratory soil specimen, *Soils and Foundations* 53(4), 510-524.

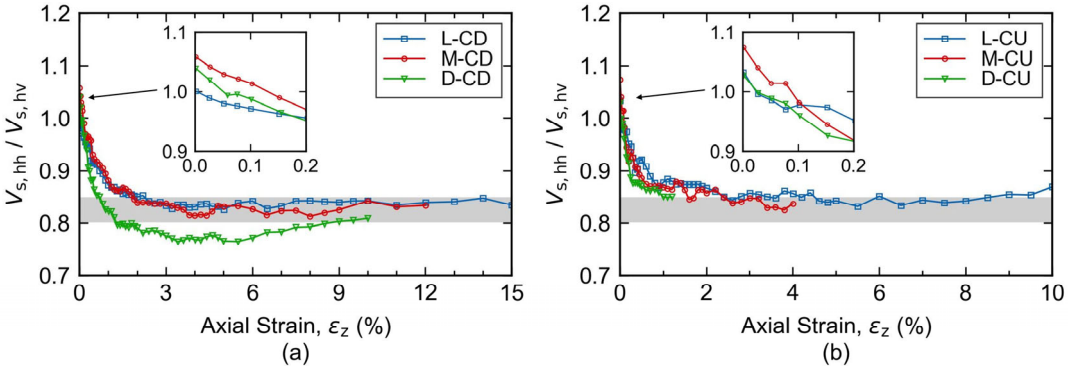

Figure 7. Evolution of S-wave velocity ratio ($V_{s,hh}/V_{s,hv}$) with axial strain (ε_z) during triaxial compression.